UNIVERSIDADE DE SÃO PAULO

INSTITUTO DE FÍSICA
CAIXA POSTAL 20516
01498 SÃO PAULO - SP
BRASIL

PUBLICAÇÕES

IFUSP/P-949

QUANTUM SIGNATURE OF A PERIOD-DOUBLING BIFURCATION AND SCARS OF PERIODIC ORBITS

C.P. Malta
Instituto de Física, Universidade de São Paulo

M.A.M. de Aguiar and A.M. Ozorio de Almeida
Instituto de Física, Universidade de Campinas
Caixa Postal 6165, 13081 Campinas, SP, Brazil

Novembro/1991

QUANTUM SIGNATURE OF A PERIOD-DOUBLING BIFURCATION AND SCARS OF PERIODIC ORBITS

C P Malta,

Instituto de Fisica, Universidade de Sao Paulo,

CP 20516, 01498 Sao Paulo, SP, Brazil

M A M de Aguiar and A M Ozorio de Almeida

Instituto de Fisica, Universidade de Campinas,

CP 6165, 13081 Campinas, SP, Brazil

ABSTRACT

The density of states is numerically calculated for a non-integrable Hamiltonian whose shortest periodic orbit family undergoes a period-doubling bifurcation in the energy interval considered. Smoothing the density using a suitable width δE, oscillations are observed due to only the family of shortest period or also its period-doubling. The period-doubling resonance results in a higher average amplitude of the corresponding spectral oscillations than for the primitive orbit. The main periodic families produce strong scars in the wave intensities. Projections of the Husimi distributions also exhibit scars that are, however, not so clear.

1. Introduction

In the last two decades a great amount of work has been done to understand the implications of the Gutzwiller trace formula (Gutzwiller 1971) in a number of situations. The main difficulty resides in the intrinsic structure of the trace formula, which connects the semiclassical density of states to a sum over all the periodic orbits of the associated classical problem. If the exact spectrum is usually hard to obtain, so is the totality of the classical periodic orbits. The influence of the periodic orbits in the eigenstates seems to be even more complex. Scars were first reported by Heller (1984) in the individual eigenstates of the Bunimovich billiard , and a theory was proposed in terms of the averaged local density of states (Heller 1986). More accurate results were then obtained by Bogomolny (1988) for the probability density in the coordinate representation. Finally, Berry (1989) lifted the results of Bogomolny to the phase space via the Wigner function. All of these theories, however, rely strongly on energy averages, and do not apply to individual states. It is therefore important to provide numerical examples of the scarring effect to guide the development of theories.

We consider here a smooth, non-integrable, Hamiltonian ("soft chaos") in contrast to the existing studies that refer to billiards and/or systems exhibiting a symbolic code for their periodic orbits. In the extreme case of a separable Hamiltonian,

the Gutzwiller formula can be shown to agree with the EBK torus quantisation conditions (Berry 1976) , which greatly simplifies the calculations. However, in the general non-integrable case, where chaos and tori are intermixed, the only known way to overcome the classical complexity is by smoothing (Balian and Bloch, 1974) the density of states. This procedure, although poorer in resolution, opens the possibility of cutting off the contribution of long periodic orbits, leading to a more treatable trace formula.

In this paper we investigate, numerically, the smoothed density of states for the smooth, non-integrable, Hamiltonian

$$H = (p_x^2 + p_y^2) / 2 + V(x, y) \quad , \qquad (1)$$

with

$$V(x,y) = (y - x^2 / 2)^2 + 0.05\, x^2 \quad . \qquad (2)$$

The simplest periodic orbits of this system have been extensively studied by Baranger and Davies (1987). This potential (codename NELSON) has a minimum at zero energy , and due to the reflexion symmetry in both x and p_x , the plane $x = 0$, $p_x = 0$ is an invariant plane in the phase space. Since the potential is harmonic along this plane, it is foliated by a family of "VERTICAL" (y-direction) oscillations of constant period $\tau = 2\pi / \sqrt{2}$.

According to the numerical study of Baranger and Davies (1987), this is the family of orbits with the shortest period in the energy interval (0.0 , 0.300) . In this interval, the vertical family undergoes three main bifurcations : a period-quadrupling at $E \simeq 0.019$, a period-tripling at $E \simeq 0.077$, remaining elliptic in both cases, and finally, a period-doubling at $E \simeq 0.136$, then becoming weakly hyperbolic. (We shall call these bifurcated families $V4$, $V3$ and $V2$, respectively.) These families have the shortest periods in the above mentioned energy interval. Another important family of this system is the "HORIZONTAL" family, so called because it starts out as a harmonic oscillation in the x-direction. Its period is always greater than the period of $V4$, and in that energy interval it undergoes two consecutive isochronous bifurcations (Aguiar and Malta 1988, Baranger and Davies 1987), one of the generated families being elliptic.

Our purpose in this paper is to identify the signature of some of these families in the quantum spectrum and eigenfunctions, including the classical phenomenon of bifurcation. This will be done by controlling the smoothing of the spectral density, as in the previous work of Malta and Ozorio de Almeida (1990). We also present the Husimi (1940) distributions projected on both (x, p_x) and (y, p_y) planes. These projections may provide information about the scarred states but, in order to obtain fine details, a long computation time is required. The wave intensities, on the other hand, can be calculated with very good precision and much less

effort.

This paper is organised as follows : in section 2 we present the smoothed density of states and show the signature of the classical orbits and bifurcations in its (discrete) Fourier transform, using Gaussian windows (Harris 1978). In section 3 we show scars of periodic orbits in the averaged wave intensities and in the Husimi distributions. The conclusion is given in section 4.

2. The smoothed density of states

The eigenvalue problem of the NELSON quantum system ,

$$H\,\psi_i(x,y) = E_i\,\psi_i(x,y) \ ,$$

was solved using the expansion

$$\psi_i(x,y) = \sum_{N=0}^{M} {\sum_{n=0}^{N}}' \ C_i^{n,N-n}\,\phi_n(x)\,\phi_{N-n}(y) \ , \qquad (3)$$

where $\phi_n(x)$ and $\phi_m(y)$ are the eigenfunctions of the one-dimensional harmonic oscillator Hamiltonians H_x and H_y ,

$$H_x = p_x^2/2 + 0.05\,x^2 \ ,$$
$$(4)$$
$$H_y = p_y^2/2 + y^2 \ .$$

The prime in the summation meaning that only even n (even parity) or only odd n (odd parity) are included.

The truncation value $N = M$, in the expansion (3), is chosen according to the energy interval to be investigated , for a given $\hbar$. Semiclassical results are obtained by using a small $\hbar$, and for a given energy interval, the smaller $\hbar$ is, the larger M has to be. We used $M = 118$ and diagonalised a matrix 3600x3600 . The calculation has been done for $\hbar = 6.0\ 10^{-3}$ and $\hbar = 9.0\ 10^{-3}$, for which the level spacing of the vertical harmonic oscillator, $\hbar\,\omega_y$, is approximately $8.5\ 10^{-3}$ and $12.7\ 10^{-3}$, respectively. For the truncation value used, the eigenvalues contained in the energy interval (0,0.200) are good. The corresponding eigenfunctions are fairly good for the larger value of $\hbar$ used but are not so good for the smaller value (of course, the lower the eigenvalue, the better the corresponding eigenfunction).

The density of states (histograms), as a function of the energy E, has been calculated in the above energy interval , with various degrees of smoothing. These densities have been Gaussian smoothed, with half width δE ,in order to eliminate spurious fluctuations that arise when the number of states contained in δE is small.

According to the periodic orbit theory, the density of states may be separated in two terms (Berry 1983),

$$d(E) = d_{av}(E) + d_{osc}(E) \ , \qquad (5)$$

where $d_{av}(E)$ is the average density of states (the so called Weyl term) corresponding to zero period orbits, and $d_{osc}(E)$ is the oscillatory term which incorporates the contribution of the periodic orbits of period greater than zero. The contribution to $d_{osc}(E)$ of the lowest period orbits may be analysed numerically, by appropriately choosing the value of δE used in the calculation. As the vertical family has the lowest period, $d_{osc}(E)$ will exhibit no oscillations, as $\hbar \to 0$, if $\delta E > \hbar\ (\omega_y = \sqrt{2})$ (for small values of $\hbar$, there will be no oscillations only if δE is fairly larger than $\hbar\ \omega_y$). In order to observe the contribution of the periodic family $V2$, resulting from a period-doubling bifurcation of the vertical family, δE must be smaller than $\hbar\ \omega_y/2$. For δE slightly smaller than $\hbar\ \omega_y/4$, in the energy interval under consideration, $d_{osc}(E)$ will have contributions of the vertical family and of all the periodic families resulting from a period n-upling bifurcation, $n \leq 4$, of this vertical family, i e families $V2$, $V3$ and $V4$.

The resulting smoothed level density for $\hbar = 6.0\ 10^{-3}$, using $\delta E = 1.0\ 10^{-3}$, is displayed in figure 1, and for $\hbar = 9.0\ 10^{-3}$, using $\delta E = 2.0\ 10^{-3}$, is displayed in figure 2. It should be mentioned that these densities were obtained numerically, at energy points separated by $1.0\ 10^{-4}$, and a line was drawn joining consecutive points.

The term $d_{osc}(E)$ is obtained by subtracting the Weyl term, $d_{av}(E)$, from the level density $d(E)$. The Weyl term has been

obtained numerically, using $\delta E = 40.0\ 10^{-3}$ (see figure 3). It should be mentioned that, for the NELSON potential, the Weyl term may be calculated analytically and it is a linear function of E (in fact, this linear behaviour of $d_{av}(E)$ is used to verify the appropriateness of the truncation value, $N = M$, for the energy interval under investigation). The ratio of the angular coefficients of the $d_{av}(E)$ terms displayed in figure 3 is equal to the ratio of the corresponding $\hbar^{-2}$, in agreement with the analytical result.

In figures 4 and 5 we display the term $d_{osc}(E)$, obtained by subtracting the corresponding Weyl term in figure 3, from $d(E)$ in figures 1 and 2, respectively. In the semiclassical periodic orbit theory, the oscillations exhibited by $d_{osc}(E)$ in figures 4 and 5, should be due to the contributions of the periodic orbits with period up to $2\pi\ \hbar/\delta E$. The δE value used, for both values of $\hbar$, is smaller than $\hbar\ \omega_y/4$, therefore, the vertical orbit and the orbits of $V2$, $V3$ and $V4$ (plus all their mth repetitions for which $m\ \tau \leq 2\pi\ \hbar/\delta E$) should be contributing to those oscillations. In the energy region after the period-doubling bifurcation has ocurred, the main contribution should come from $V2$, as the vertical orbit becomes hyperbolic after this. Nevertheless, the contribution of the vertical orbit remains significant even after its period-doubling bifurcation, because its instability sets in very slowly. The contributions of $V3$ and $V4$ are not so significant since, as already mentioned, the vertical orbit remains stable at

those bifurcations.

In order to verify all those facts mentioned above, we made a Fourier analysis of $d_{osc}(E)$ in figures 4 and 5, using Gaussian windows (Harris 1978). Considering the whole energy interval (a single window), the Fourier analysis shows that, in both cases, the main frequency contributing is $2\ (\hbar\ \omega_y)^{-1}$, but the frequency $(\hbar\ \omega_y)^{-1}$ still contributes significantly (see figures 6 and 7). As for the frequencies $3\ (\hbar\ \omega_y)^{-1}$ and $4\ (\hbar\ \omega_y)^{-1}$, their contributions are small, as expected (it should be mentioned that the single window Fourier analysis does not exhibit peaks at these frequencies if $(\hbar\ \omega_y/3) < \delta E < (\hbar\ \omega_y/2)$.

3. Averaged wave intensities and Husimi distributions

The classical structure, underlying the wave fuctions in the semiclassical limit, may be observed through the wave intensities, $|\psi_i(x,y)|^2$, and also through the Husimi (1940) distributions, $h_i(x,y,p_x,p_y)$ (a Gaussian smoothed version of the Wigner distribution).

We are interested in detecting the existence of scars due to the vertical family, and its period n-upling bifurcations. Therefore, we have calculated the state density distribution averaged over y, given by

$$\rho_i(x) = \int |\psi_i(x,y)|^2 dy =$$

$$\simeq \sum_{N=0}^{M} \sum_{N'=0}^{M} \sum_{n=0}^{N} ' \; C_i^{n,N-n} \; C_i^{N'-N+n,N-n} \; \phi_n(x)\; \phi_{N'-N+n}(x). \quad (6)$$

Only even parity states may exhibit a scar due to the vertical family as the odd parity states are zero at the origin. Both the period-doubled and the period-quadrupled orbit are symmetric librations, while the period-tripled orbits are symmetric rotations (there is also a pair of period-tripled asymmetric librations which are hyperbolic).

The averaged wave intensity, $\rho_i(x)$, for the eigenstates corresponding to the eigenvalues 0.1234, 0.0401 and 0.1195 are shown in figures 8,9 and 10, respectively ($\hbar = 9.0\ 10^{-3}$). The scar seen in figure 8 is immediatly identified as due to the vertical family. The set of states exhibiting this scar are separated in energy by $\hbar\ \omega_y$. The scar seen in figure 9 can also be easily identified as due to the horizontal family since it belongs to a set of states that acquire a pair of oscillations as the energy is increased, the energy difference of the first two states being approximately $2\hbar\ \omega_x$. The scar seen in figure 10 is exhibited by a set of states separated in energy by $\hbar\ \omega_y$. To each member of this set there corresponds a member of the set exhibiting the vertical orbit scar (figure 8). In order to confirm the above

analysis we also calculated the projected Husimi distribution for the eigenstates, as the Husimi distribution , being a function of four variables is very hard to visualize (and to compute).

The projections of $h_i(x,y,p_x,p_y)$ on a canonically conjugate pair , (x,p_x) or (y,p_y) are obtained by integrating over the other pair. Let $|z_x\rangle$ and $|z_y\rangle$ be the usual coherent states for the oscillators of eq. (4), with

$$z_x = (\sqrt{0.1}\, x + i\, p_x/\sqrt{0.1})/\sqrt{2} \quad ,$$
$$z_y = (\sqrt{2}\, y + i\, p_y/\sqrt{2})/\sqrt{2} \quad . \qquad (7)$$

Then, the Husimi distribution h_i can be written as

$$h_i = | \langle \psi_i | z_x\, z_y \rangle |^2 \simeq | \sum_{N=0}^{M} \sum_{n=0}^{N}{}' \; C_i^{n,N-n} \langle n|z_x\rangle \langle N-n|z_y\rangle |^2, \qquad (8)$$

where

$$\langle n|z\rangle = (z/\hbar)^n \exp(-z\, z^*/2\hbar)/\sqrt{n!} \quad . \qquad (9)$$

The projection of h_i on the plane (x,p_x) is given by

$$h_i(z_x) = \sum_{N=0}^{M} | \sum_{n=0}^{M-N}{}' \; C_i^{n,N} \langle n|z_x\rangle |^2 \quad . \qquad (10)$$

The projection on the plane (y,p_y) is given by a similar expression .

The projections $h(z_x)$ and $h(z_y)$ were calculated for a large number of eigenstates. For the eigenstates exhibiting the scar shown in figure 8, the Husimi projection $h(z_x)$ (figure 11) has a single, narrow, peak at the origin. For the eigenstates exhibiting the scar shown in figure 10, the Husimi projection $h(z_x)$ also has a single (broader) peak at the origin (figure 12). Now, for the former type of eigenstates, the Husimi projection $h(z_y)$ exhibits peaks along the y-axis only (see figure 11), while for the latter type of eigenstates,it also exhibits peaks away from the the y-axis (see figure 12), indicating that this set of states has some quanta (an even number, due to the $x \leftrightarrow -x$ symmetry) in the "horizontal" direction (remember that classically the orbit is a horizontal oscillation only at very low energies). In figure 13 we display the projected Husimi distributions for the eigenstate whose wave intensity is shown in figure 9 (horizontal family).

Following Mahoney (1987), we associate to each pair of eigenstates , n,n', a period, and a mean energy, defined as

$$\tau_{n,n'} = k\, 2\pi\, \hbar/|E_n - E_{n'}| \quad ,$$
$$E_{n,n'} = (E_n + E_{n'})/2 \quad , \qquad (11)$$

respectively. We may then construct $E\tau$ plots as in the classical case (Baranger and Davies 1987, Aguiar et al 1987). In figure 14 we display the $E_{n,n+1}$ x $\tau_{n,n+1}$ plot (k=1) for the set of states exhibiting the scar of the V family (figure 8). These points lie on the vertical line $\tau = (2\pi\,\omega_y)^{-1}$, which is the (classical) $E\tau$ plot of the V family. In figure 14 we also display the $E_{n,n'}$ x $\tau_{n,n'}$ plot (k=2) associated to the energy separation between the states in the set above and the corresponding state in the set characterized by the scar shown in figure 10 (points on the other curve). The continuous curve that would fit these points has approximately the same slope of the $E\tau$ plot of the (classical) "horizontal" family (Baranger and Davies, 1987), but would lie above it. The $E_{n,n+1}$ x $\tau_{n,n+1}$ plot for the set of states exhibiting the scar of the horizontal family (figure 9) lies closer to the classical horizontal family plot, but does not coincide with it. It should be mentioned that this plot tends to the classical one as $\hbar$ gets smaller.

4. Final discussion

In the previous work of Malta and Ozorio de Almeida (1990), all attention was directed at the effect, on the spectrum, of the first iteration of the shortest periodic orbit. The above results extend our view to higher iterations and their bifurcation resonances. The computational difficulty that arises is that the

number of levels within these higher frequency oscillations of the spectrum is smaller, so that even Gaussian smoothing may become unreliable.

It is easy to calculate the amplitude of the oscillations for each of the periodic orbits viewed through the Gaussian window employed in analysing the spectrum. Figure 15 shows the Gutzwiller amplitudes, with the amplitude of the second repetition of the V orbit exhibiting a singular peak at the period-doubling bifurcation point ($E \simeq 0.136$). The theory of Ozorio de Almeida and Hannay (1987) substitutes this singularity by a finite peak, but the general picture is the same. It is, therefore, satisfying that figures 4 and 5 indeed confirm the prediction that the period-doubled orbit has a larger average amplitude than the primitive one. It should be noted that the spectrum was not resolved to the point of distinguishing the stable period-doubled orbit from the second repetition of the unstable vertical orbit. Of course, it would be worthwhile to determine the Fourier amplitudes of the spectrum, for narrow energy windows, as a function of the centre of the window. However, though we can discern the broadened peaks for V and $V2$ (figure 16) the amplitudes were found to fluctuate erratically. A consistent picture of the energy evolution of the oscillations requires that the spectrum be obtained for considerably smaller value of Planck's constant, so that the density of states within each oscillation exhibits less fluctuation. We hope to be able to reveal the detailed behaviour of the orbit amplitude as a function

of the energy in future calculations.

It is not only in the analysis of the spectrum that it is important to understand the features due to the classical bifurcations, which are avoided in the common use of homogeneous Hamiltonians. In the scarred states, the important qualitative features may be traced to different origins within the regular region at low energies. Thus, we find that the sequence of states corresponding to the vertical orbit(figure 8), with only zero-point horizontal oscillation, survive neatly into the unstable region with no qualitative change in shape (confirming a previous private communication of Leboeuf and Saraceno). This is not the case of the next symmetric sequence of states (two horizontal quanta, scar of the type shown in figure 10). Though there is still a regular sequence in the chaotic region, with the wave intensity more spread out than in the proper scars (figure 10), the peak at the periodic orbit grows at the expense of the other maxima, while becoming thinner (figure 17). We can thus understand the, at times bewildering, number of "scarred states" as originating in torus states, as some bifurcation parameter is varied. The concentration of the states at the periodic orbit, while mantaining a spread around it, is compatible with the hypothesis of homoclinic quantisation proposed by Ozorio de Almeida (1989). For $\hbar = 6.0\ 10^{-3}$, the picture is the same and, besides, because $\hbar$ is smaller, the scars are more neat and there are other symmetric sequences corresponding to four and six "horizontal" quanta.

Acknowledgements

We acknowledge partial financial support of CNPq (Conselho Nacional de Desenvolvimento Científico e Tecnológico). MAMA and AMOA are also partly supported by FINEP and FAPESP.

CPM acknowledges the kind hospitality of the MIT Center for Theoretical Physics, specially Profs. Michel Baranger and John Negele. This work was partially supported by DOE (department of Energy) under contract # DE-AC02-76ER03069.

References

de Aguiar M A M and Malta C P 1988 *Physica* **D30** 413

de Aguiar M A M, Malta C P, Baranger M and Davies K T R 1987 *Ann. Phys., NY* **180** 167

Balian R and Bloch C 1974 *Ann. Phys., NY* **85** 514

Baranger M and Davies K T R 1987 *Ann. Phys., NY* **177** 330

Berry M 1976 *Proc. Roy. Soc.London* **A349** 101

1983 *Chaotic Behaviour of Deterministic Systems (Les Houches, 1981)* Session 36, eds G Ioss, R G Helleman and R Stora (Amsterdam: North-Holland) p 171

1989 *Proc. Roy. Soc.London,* **A423** 219

Bogomolny E 1988 *Physica* **31D** 169

Gutzwiller M C 1971 *J. Math. Phys.* **8** 1979

Harris Frederic J 1978 *Proc. of the IEEE* **66** 51

Heller E 1984 *Phys. Rev. Lett.* **53** 1515

1986 *Quantum Chaos and Statistical Nuclear Physics,* eds T H Seligman and H Nishioka, *Lect. Notes in Physics* **273** 162 (Springer)

Husimi K 1940 *Proc. Phys Math Soc. Jpn* **22** 264

Mahoney, J H 1987, *PhD Thesis,* MIT, Cambridge, USA

Malta C P and Ozorio de Almeida A M 1990 *J. Phys. A: Math and Gen.* **23** 4137

Ozorio de Almeida A M 1989 *Nonlinearity* **2** 519

Ozorio de Almeida A M and Hannay J H 1987 *J. Phys. A: Math. and Gen.* **20** 5873

Figures Caption

Fig.1 Gaussian smoothed $d(E)$, for $\hbar = 6.0\ 10^{-3}$, using δE=1.0 10^{-3}.

Fig.2 Gaussian smoothed $d(E)$, for $\hbar = 9.0\ 10^{-3}$, using δE=2.0 10^{-3}.

Fig.3 The Weyl term, $d_{av}(E)$, for $\hbar = 6.0\ 10^{-3}$ (steeper curve) and for $\hbar = 9.0\ 10^{-3}$.

Fig.4 $d_{osc}(E)$ for $\hbar = 6.0\ 10^{-3}$, using $\delta E = 1.0\ 10^{-3}$.

Fig.5 $d_{osc}(E)$ for $\hbar = 9.0\ 10^{-3}$, using $\delta E = 2.0\ 10^{-3}$. One should note that $\tau_{max} = 2\pi\ \hbar/\delta E$ is smaller here than in figure 4, resulting in smaller frequency and amplitude of the fluctuations.

Fig.6 Single Gaussian-window Fourier analysis of $d_{osc}(E)$ in Fig 4.

Fig.7 Single Gaussian-window Fourier analysis of $d_{osc}(E)$ in Fig 5.

Fig.8 $\rho_i(x)$ for the eigenstate with $E = 0.1234$, $\hbar = 9.0\ 10^{-3}$.

Fig.9 $\rho_i(x)$ for the eigenstate with $E = 0.0401$, $\hbar = 9.0\ 10^{-3}$.

Fig.10 $\rho_i(x)$ for the eigenstate with $E = 0.1195$, $\hbar = 9.0\ 10^{-3}$.

Fig.11 The Husimi projections $h_i(z_x)$ and $h_i(z_y)$ for the state in Fig 8.

Fig.12 The Husimi projections $h_i(z_x)$ and $h_i(z_y)$ for the state in Fig 10.

Fig.13 The Husimi projections $h_i(z_x)$ and $h_i(z_y)$ for the state in Fig 9.

Fig.14 $Ex\tau$ plots (see description in the text).

Fig. 15 The Gutzwiller amplitudes. The continuous line is the second repetition of V ($2V$), long dash is V, short dash is $V2$ and dot-dash is the sum of $V2$ and $2V$.

Fig. 16 Fourier amplitude, as function of E, using Gaussian windows of width $\Delta E = 0.05$. The continuous line is the amplitude of $V2$ and the dashed line is the amplitude of V.

Fig. 17 $\rho(x)$ for an eigenstate in the chaotic region ($E = 0.1861$), well above the period-doubling bifurcation ($\hbar = 9.0\ 10^{-3}$).

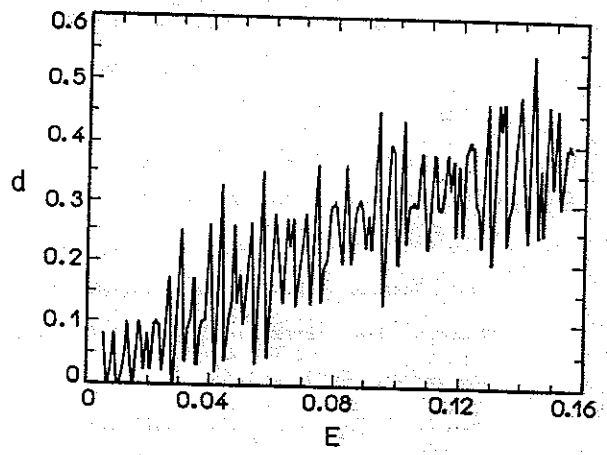

Figure 1

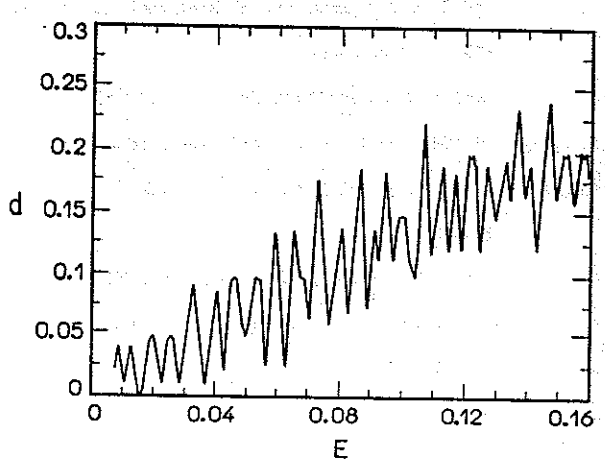

Figure 2

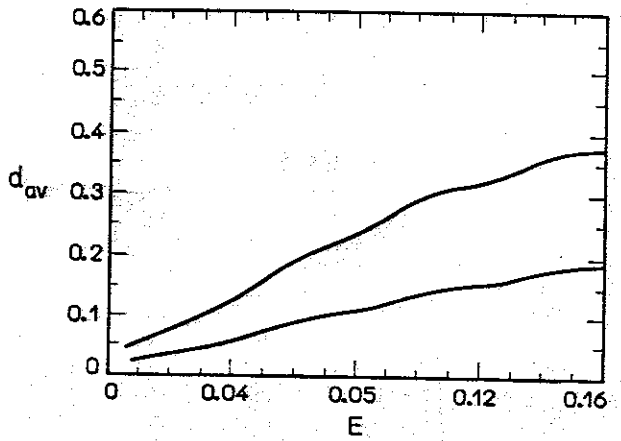

Figure 3

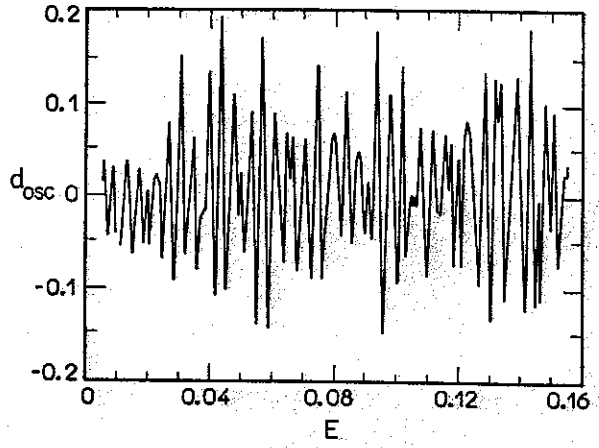

Figure 4

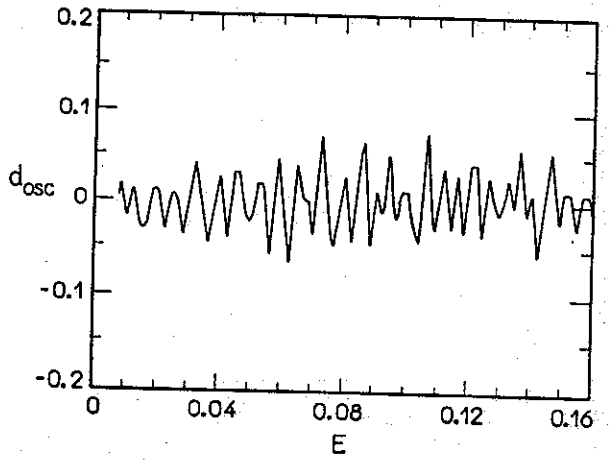

Figure 5

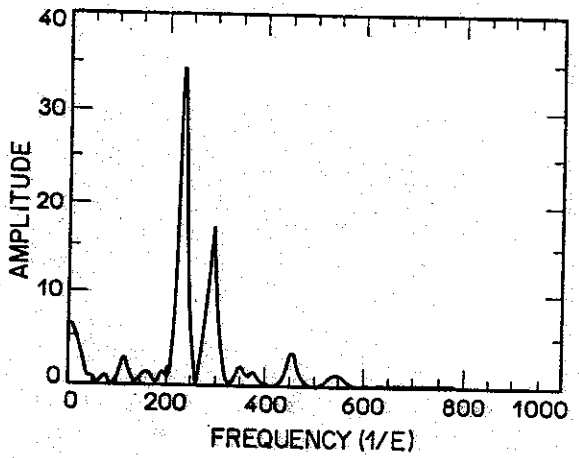

Figure 6

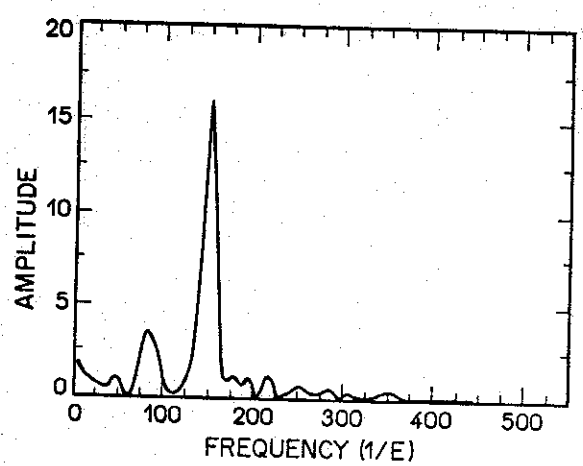

Figure 7

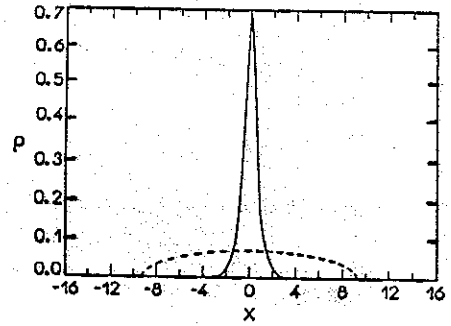

Figure 8

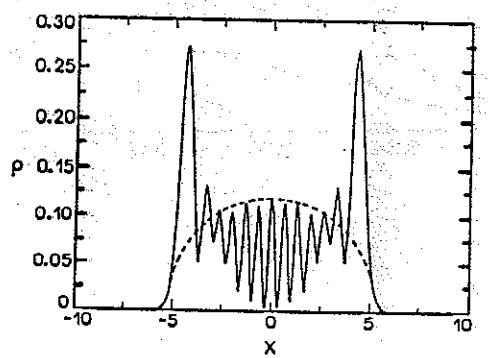

Figure 9

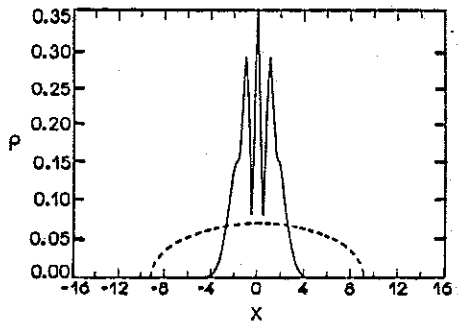

Figure 10

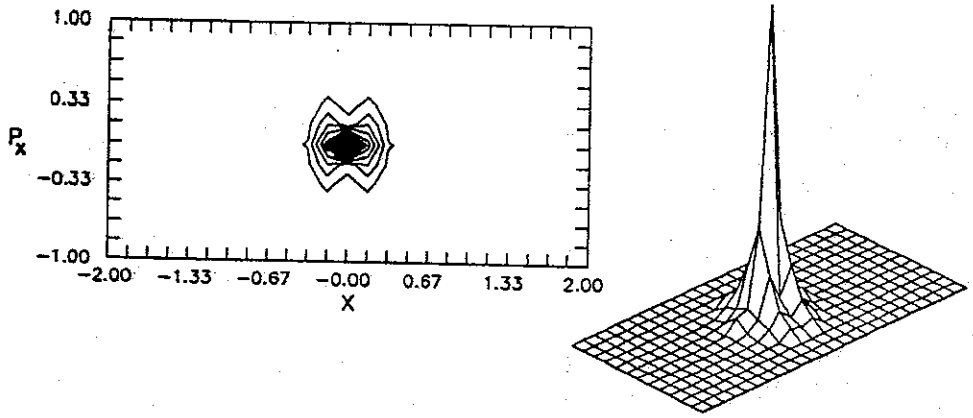

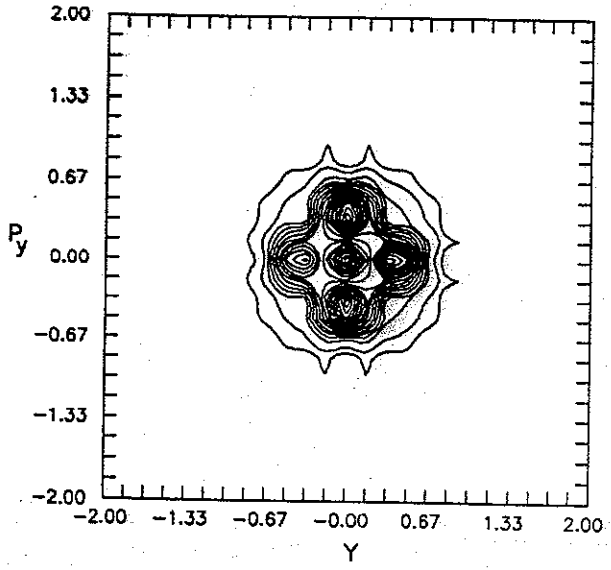

Figure 11

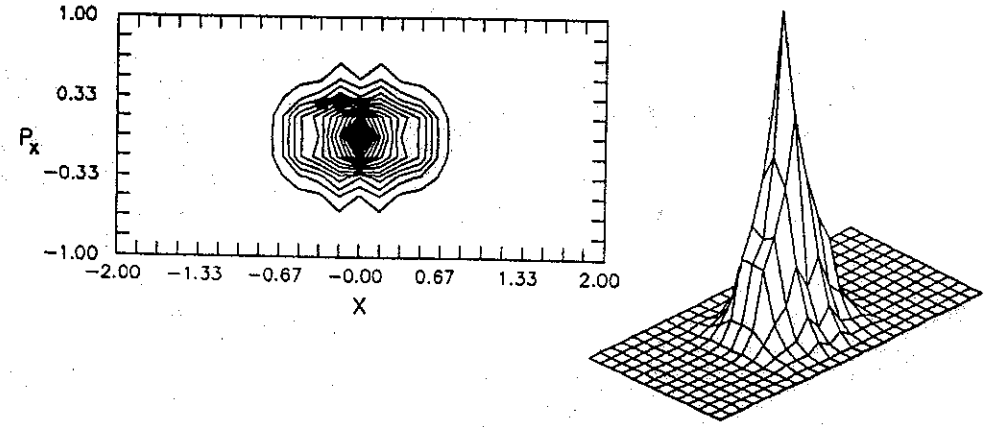

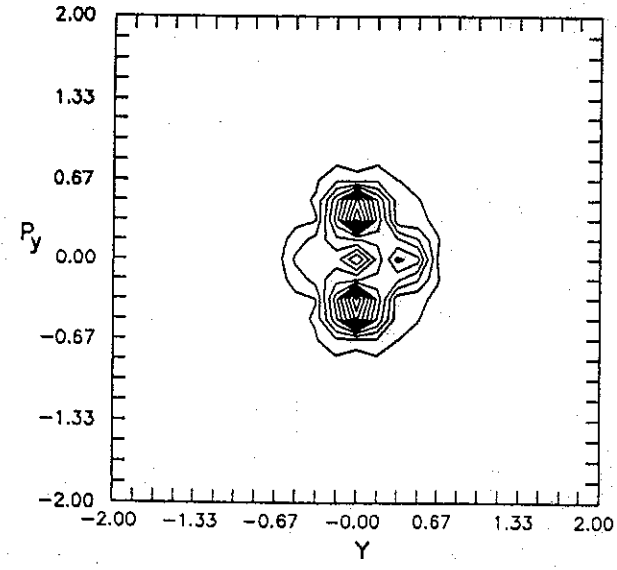

Figure 12

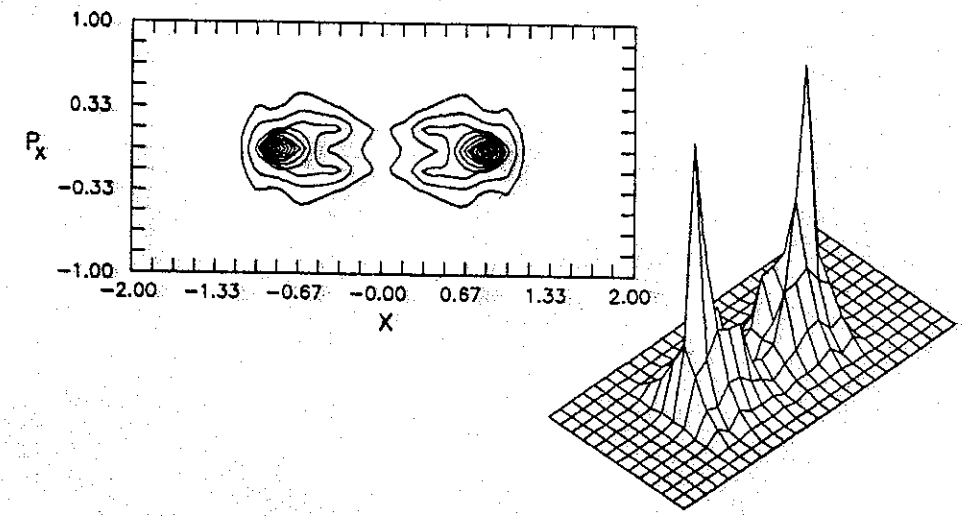

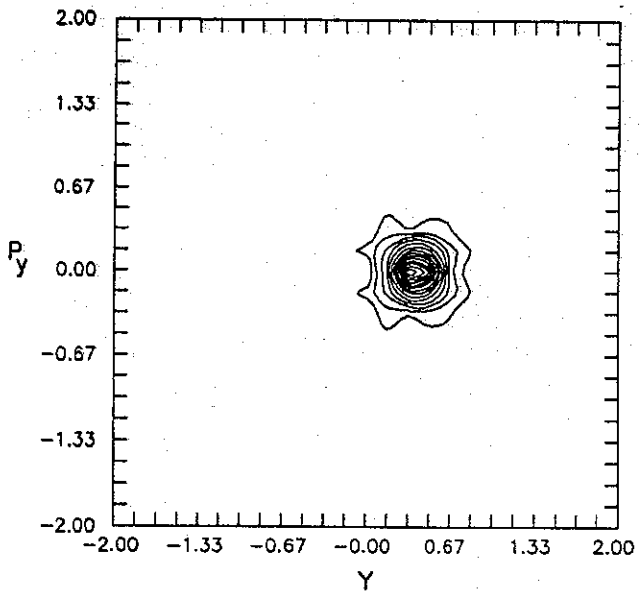

Figure 13

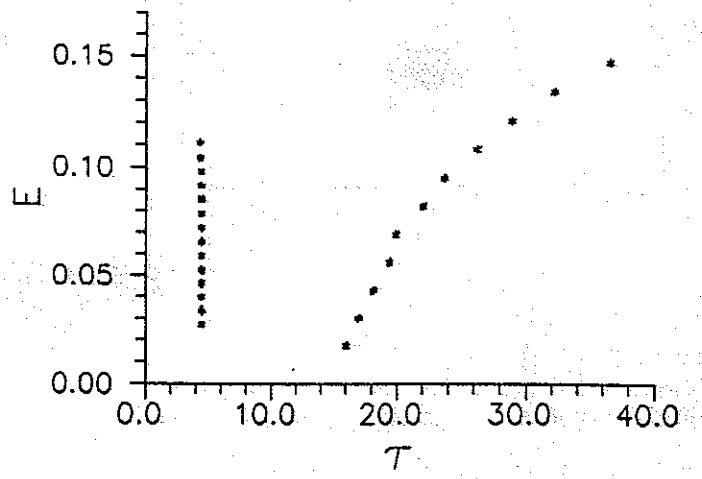

Figure 14

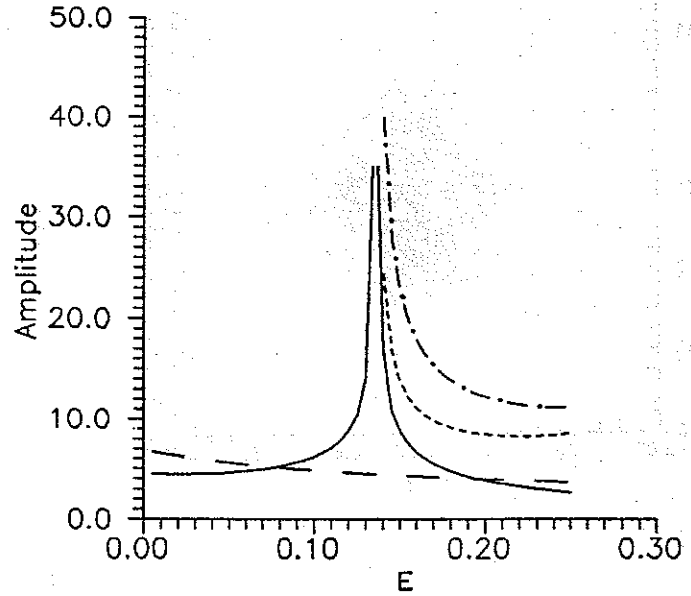

Figure 15

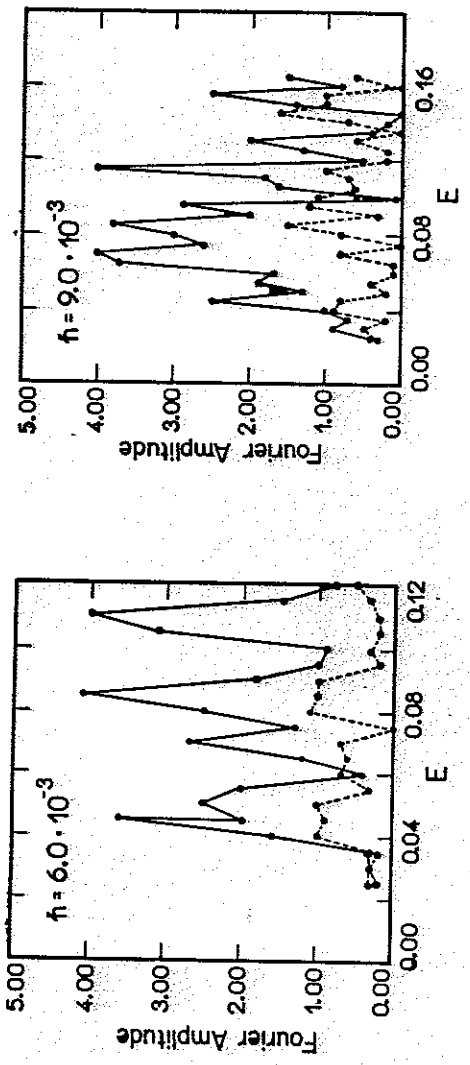

Figure 16

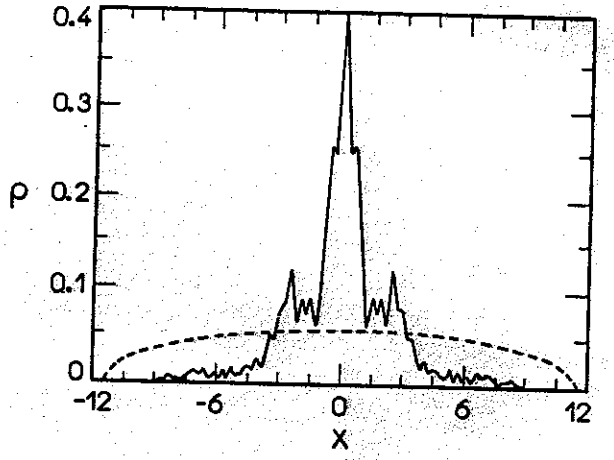

Figure 17